*Journal of Sound and Vibration* (1997) **206**(5), 663–684

# A STUDY OF THE INITIAL DECAY RATE OF TWO-DIMENSIONAL VIBRATING STRUCTURES IN RELATION TO ESTIMATES OF LOSS FACTOR

L. Wu, A. Ågren and U. Sundbäck

*Acoustics Group, Luleå University S*-971 87 *Luleå, Sweden*

(*Received* 31 *August* 1995, *and in final form* 2 *June* 1997)

The aim of this study was to obtain a better understanding of the process of the initial decay of energy in relation to the estimates of damping loss factor; to investigate the spatial variation of the initial decay rate in order to obtain more reliable estimates of damping loss factor from the decay rate method; and to compare the spatial averages and spatial variation of damping loss factor between the decay rate method and the power input method. The initial decay rate of energy was experimentally investigated on uniform plates. The energy mean free path time was introduced as a factor to characterize the lower limit of a decay interval for fitting an initial decay slope, and to determine the initial point of a decay curve. It is concluded that the initial decay slopes can sometimes be determined within a very short decay interval (e.g., less than 10 dB) provided that the corresponding time interval is larger or much larger than the energy mean free path time. Additionally, the effect of the direct field on the initial decay can be ignored provided that the response point is far enough from the drive point. An analysis of the spatial variation of initial decay rate showed that an increase in the number of modes per band, and light and moderate damping can reduce the spatial variation. High damping may increase the spatial variation. For a frequency band with more modes, fewer response points need to be used to obtain a stable estimation of spatial variance. It was confirmed that the damping loss factor determined from the decay rate method was in general in good agreement with the power input method. The comparison of the spatial variances of damping loss factor between the two methods showed that the decay rate method gives a more reliable estimate of the damping loss factor of the plates. It is concluded that the decay rate method is to be preferred to the power input method when determining the damping loss factor of a system.


## 1. INTRODUCTION

Knowledge of the damping characteristics of structure components is essential in all types of dynamic analyses including the statistical energy analysis (SEA). Since damping does not refer to a unique physical phenomenon, it is difficult to predict damping in general [1–3]. Experimental methods constitute therefore in many cases the only appropriate approach. The most common methods for determining the damping loss factor experimentally can be divided into three groups [2–4]: (i) the decay rate method, (ii) the power input method, and, (iii) the experimental modal analysis method.

Of the three methods, the power input method has the advantage of being closely connected with the definition of structural losses [3]. Practical use of the power input method is, however, limited to uniform structures or the structures where the mass density distribution is known. In addition, this method may be subject to error associated with spectral estimation of input power.

0022–460X/97/400663 + 22 $25.00/0/sv971131 

There is no general way of computing frequency-band values from the modal loss factors, except in the cases of equal modal damping, equal modal energy and equal power flow into each mode [3, 5, 6]. Therefore, in general with regard to frequency band average loss factors, the power input method is not comparable with the techniques of experimental modal analysis.

The consistency between the power input method and the decay rate method, in structural acoustics, has been argued for some time in the literature, particularly with regard to the selection of decay slope [5–9]. Since energy decay curves often appear as dual-slope or multiple-slope curves, it is essential to know which part of the decay curves should be used to estimate damping loss factors that are consistent with the results from the power injection method. It was concluded by Jacobsen [3] that, in principle, with the condition that the driving points are the same, the power input method is equivalent to the decay rate method provided the initial part of the vibration energy decay curve is used. He experimentally verified this consistency relationship with various structure configurations.

Theoretically, the initial decay rate should be determined by fitting a straight line to a decay interval which is as short as possible [3]. However, an arbitrarily short interval may not be appropriate since the change of vibration energy in a system from one state to another takes place during a finite time. Another difficulty met when determining the initial decay slope in structures is the determination of the starting point of a decay curve since the initial decay stage is influenced by both the direct and the reverberant fields.

From one perspective regarding the consistency relationship between the decay rate and the power input methods, the initial decay rate is also related to the location of the excitation points and the measurement points. This means that the initial decay rate has a spatial variation. To obtain a reliable estimate of a spatial average of initial decay rate, it is necessary to investigate its spatial variation. It has been pointed out that the decay rate method can give a fair estimation of loss factor without any spatial averaging compared to the power input method [3]. It is still unclear, however, whether the decay rate method yields less spatial variance in the estimate of damping loss factor than the power input method does when a certain number of driving points and measurement points are used. If this is the case, then the initial decay rate can be used as a benchmark to adjust the estimation of the energy term in the power input method and the decay rate method will be preferred to the power input method when determining the damping loss factor of a system.

The purposes of the study are, therefore, as follows: (i) to define the lower limit of the time interval for the initial decay slope and to specify the starting point of an energy decay curve; (ii) to verify the consistency relationship of damping loss factor between the decay rate method and power input method; (iii) to investigate the spatial variance of initial decay rate; (iv) to compare the variance of damping loss factor from the decay rate method and the power input method. The study is based on experimental investigations of uniform and rectangular plates.

## 2. THEORETICAL BACKGROUND OF CONSISTENCY RELATIONSHIP BETWEEN THE DECAY RATE METHOD AND THE POWER INPUT METHOD

For a system, the consistency between the decay and the power input method [3] can be expressed as

$$\eta = \gamma/27{\cdot}3f = P/\omega E, \tag{2.1}$$

where $\eta$ is the frequency band averaged damping loss factor, $P$ is the steady state value of input power, $E$ is the steady state value of energy, $\omega = 2\pi f$ is the center frequency of the band and $\gamma$ is the initial decay rate (dB/s) of the system at time $t = 0$ when the input power is suddenly cut off and is given as

$$\gamma = \mathrm{d}[10 \log E(t)]/\mathrm{d}t \,|_{t=0}, \tag{2.2}$$

where $E(t)$ is the time dependent energy averaged over a short time [10]. This short time may be related to the energy mean free path time that will be discussed afterwards.

The middle and right terms in equation (2.1) denote the decay rate method and the power input method respectively. Equations (2.1) and (2.2) show that, for the frequency band average damping loss factor, the decay rate method is equivalent to the power input method provided the initial decay rate is used. Furthermore, the time $t = 0$ in equation (2.2) implies that the initial decay rate is to be determined in a state when the steady state energy level exhibits little change, and light and moderate damping conditions are assumed [3].

In the steady state, the frequency band average damping loss factor determined from the power input method in equation (2.1) can be expressed by the modal damping and modal energy as [3, 5, 7]

$$\eta = \sum_{i=1}^{N} \eta_i E_i / E \qquad \text{for } i = 1, 2, 3, \ldots, N, \tag{2.3}$$

where $E_i$ and $\eta_i$ are the modal energy and modal loss factor of the $i$th mode in the frequency band. This implies that the frequency band average of damping loss factor determined from the power input method depends on the distribution of driving points and measurement points. In terms of the consistency relationship between the power input method and the decay rate method, this distribution also affects the frequency band average of damping loss factors determined from the decay rate method.

## 3. EXPERIMENTS

### 3.1. DECAY MEASUREMENT

In the study, measurement and analysis was carried out with an LMS (Leuven Measurement & Systems) CADA-x, FFT-based measurement system with eight channels. With this system, vibration energy decay was measured, for random noise burst excitation, by digital filtering and averaging. It has been pointed out [11] that the method provides a fast and reliable way of collecting data with multiple averaging. The excitation time was varied from 30% to 60% of the total length in one time record. The excitation time used ensured that the structures were sufficiently excited at the same time as the whole decay period could be observed. With reference to the study [11], thirty averages were used to obtain the ensemble average in the decay measurements. It was assumed that this averaging number was sufficiently large to ensure the absence of noise in the decay measurements. This method requires, however, a repetition of the decay measurement for every third octave band being studied. In addition, the FFT processing in the LMS system requires that the measured frequency bandwidth be to the power of 2. Thus, the frequency bandwidths were only approximations of the corresponding third octave bands. The difference between the two types of bandwidths increases with frequency. For instance, at 500 Hz, the third octave bandwidth is 115 Hz and the actual bandwidth is 128 Hz; at 2500 Hz, the third octave bandwidth is 580 Hz and the actual bandwidth is 1024 Hz. Thus,

to ensure that the structure be excited only in the bands of interest, the excitation signal was filtered by a 1/3 octave band-pass filter set.

In addition, several other techniques for the determination of decay can be found in the literature, e.g., (i) a technique based on running time average estimates [12–14]; (ii) a technique based on the Schroeder integrated impulse response [15–17]; and (iii) a technique based on amplitude tracking in the frequency domain [11]. These techniques have the advantages of reducing both the noise and the irregularity in decay measurements. An example of a comparison of the energy decay envelopes determined from the burst random noise and the Schroeder integrated impulse methods is given in Figure 1. It is shown that the initial decay slopes derived from the two methods are very close. It is noted that the Schroeder integrated impulse method yields a much more smooth decay curve than the random noise burst method. However, a drawback of the Schroeder integrated impulse method is that the decay envelope including the time period before the cut-off of input power cannot be fully observed. The later part of the decay curve may be biased due to the influence of the insufficient spectral resolution [17], which can be seen in the figure. Thus, to study the whole process of energy decay, the random noise burst method is considered to be appropriate.

### 3.2. MEASUREMENT SET-UP

The energy decay curve and time averaged squared acceleration were measured with PCB type 353 accelerometers (2 grams each). The input power was determined by measurement of the cross-power spectrum between the force and acceleration signals captured by a (Brüel and Kjaer) type 8001 impedance head. Since phase errors between

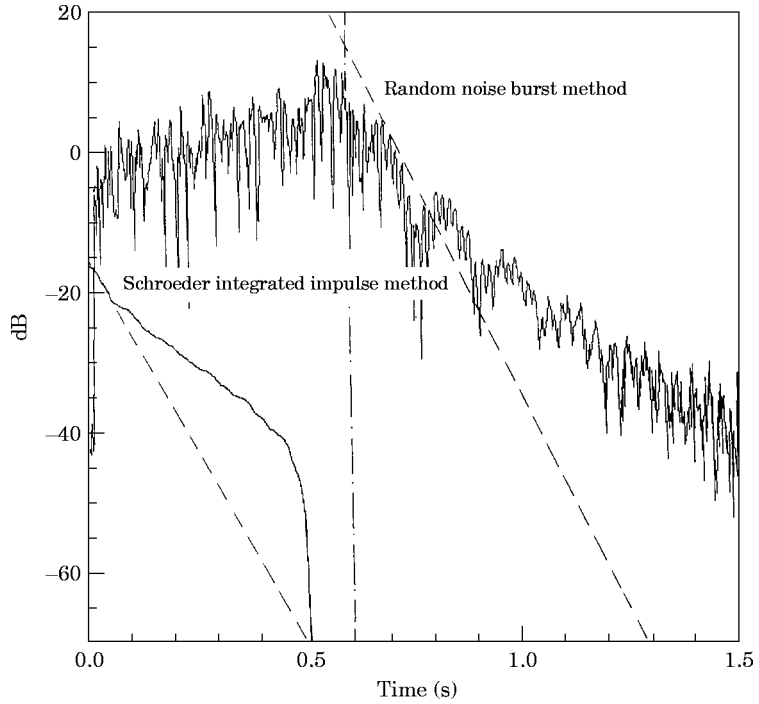


Figure 1. Comparison of decay envelopes at the third octave band of 1000 Hz, between the random noise burst method and the Schroeder integrated impulse method. The decay curve from the Schroeder integrated impulse method is shifted down by 30 dB. The measurement was carried out at a point in an undamped aluminium plate (952 × 604 × 5 mm).

the force and the acceleration signals may affect the input power [3], this problem is particularly evaluated by applying the impedance head to a free mass (about 20 grams) mounted on the impedance head and measuring the phase difference. As shown in Figure 2, the phase differences between the force and velocity signals are within $\pm 0{\cdot}2$ degrees in the frequency range of interest. This phase mismatch is considered very small. The random errors in the estimate of input power and squared acceleration due to a finite averaging time can be reduced by increasing the ensemble averaging number. In the study, the ensemble averaging number was set to 100, which will lead to a normalized random variance below 0·01 [14].

The structures were excited by a shaker with a driving rod. The measurements were carried out on the structures described in Table 1, which includes the several conditions of undamped ($\eta \approx 0{\cdot}001$), light damped ($0{\cdot}001 < \eta < 0{\cdot}01$), highly damped ($\eta > 0{\cdot}01$) plates as well as single and coupled plates. The number of randomly selected measurement and driving points on the structures are also defined in Table 1. For each of the structures tested, the measurement points and driving points were located at the same position in both the decay rate and power input methods.

## 4. SELECTION OF INITIAL DECAY SLOPE

Some typical patterns of energy decay curves in a log scale are given in Figure 3(a–d). Figure 3(a) shows an energy decay curve decaying linearly with time, which was measured in a frequency band that includes only one mode. Figure 3(b) gives in addition an approximate linear energy decay curve measured in a frequency band that includes several modes. In both cases, the decay rates are identical within a large decay interval. However, the energy decay curve may exhibit a dual-slope or a multiple-slope for a frequency band that includes more than one mode as shown in Figure 3(c). The initial decay rate determined by fitting a straight line to the first part of the decay curve will be very different to the decay rate of the rest. Modes with different decay rates and energy levels in a band may be dominant in different parts of the decay history. It is, however, not necessary that the modes in a band possess different modal damping in order to appear

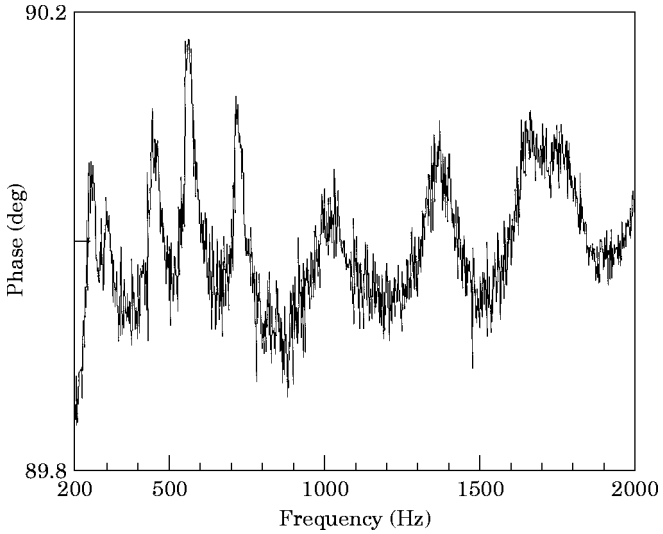


Figure 2. Phase mismatch measured between the force and velocity signals in the impedance head when a free mass (20 g) is mounted on the impedance head.

TABLE 1

*Properties of the plates tested and the number of measurement points and driving points*

| Case no. | 1 | 2 | 3 | 4 | 5 |
|---|---|---|---|---|---|
| Structure configuration | a rectangular plate 1 | a rectangular plate 1 | a rectangular plate 1 | a rectangular plate 2 | two rectangular plates coupled by three bolts |
| Material<br>Dimension ($mm^3$) | steel<br>$545 \times 460 \times 5$ | steel<br>$545 \times 460 \times 5$ | steel<br>$545 \times 460 \times 5$ | steel<br>$470 \times 409 \times 3$ | steel<br>$545 \times 460 \times 5$ and $470 \times 409 \times 3$ |
| Mass (kg) | 9·55 | 9·80 | 10·33 | 4·90 | 9·80 and 4·90 |
| Damping treatment | no additional damping | lightly damped by attaching 3 mm rubber strips to the edges of the plate | highly damped by attaching a 6 mm rubber layer to the back side of the plate | lightly damped by attaching 3 mm rubber strips to the edges of the plate | lightly damped by attaching 3 mm rubber strips to the edges of the plates |
| No. of measur. /drive points | 12/3 | 6/3 | 6/3 | 6/3 | 6/3 for each plate |

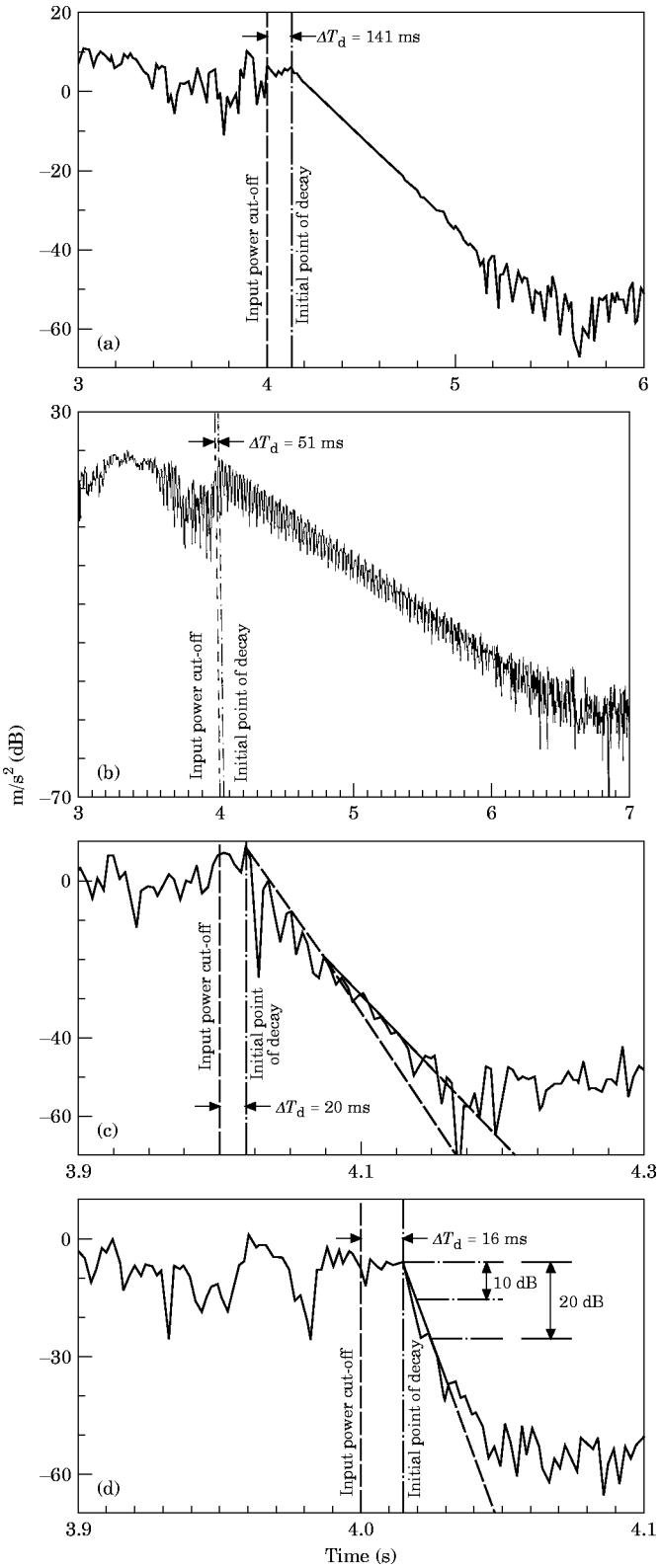


Figure 3. A typical decay envelope in a third octave band in the damped plate 1. $\Delta T_d$ : a time delay of the initial point of energy decay when the input power has been suddenly cut off. Third octave band centre frequencies (Hz): (a) 250; highly damped plate (b) 630; lightly damped plate (c) 800; highly damped plate (d) 1600; highly damped plate.

as a dual-slope or a multiple-slope. Even for modes with similar modal damping in a band, they may decay at different rates if their resonance frequencies are at the far ends of a frequency band. The reason for this is that the initial decay rate is directly proportional to the frequency as shown in equation (2.1). Of course, dissimilar modal damping at modes in a band may enhance this phenomenon. Figure 3(d) shows a decay envelope measured in a highly damped frequency band. The energy level decays dramatically within a very short time.

To fulfil the condition in equation (2.2), the initial decay rate should be determined by fitting a straight line to the energy decay curve within an interval which is as short as possible. However, it can be seen from the figures above that the initial decay slopes for different decay curves may be determined within very different decay intervals. In addition, a time delay is observed between the moment when the input power is cut off and the moment when the energy starts to decay in these figures. To clarify these two points, the process of energy decay in a structure needs to be considered.

### 4.1. STEP-WISE FUNCTION OF ENERGY DENSITY DECAY IN A VIBRATION FIELD

The decay pattern of the vibration field in a structure may be readily described in terms of the concept of energy rays [18, 19]. When the vibrational energy is a structure reaches steady state, the energy density at any observation point is comprised of two contributions. One is that from the direct field, i.e., the direct energy flow from the excitation source, and the other is that from the reverberant field, i.e., the energy flows reflected from the boundaries. When the excitation source is suddenly switched off, the steady state energy density starts to decay. The first drop of energy density at the observation point is due to the disappearance of the direct energy flow. This is not detected immediately, however, since it takes some time for the "end" of the emitted energy flow to travel from the source to the observation point. The reflected energy flows then disappear one by one as the "end" of each energy flow passes the point of observation. It can be seen that the decay of energy density in a structure appears as a series of steps in time. The lengths of the steps will seldom be identical due to the various paths of reflected energy flows, the edge scattering and diffraction of bending waves (only this type of wave is considered in the study). To make the analysis easier, however, a concept of average length of steps is introduced, which is called here the energy mean free path time.

### 4.2. ENERGY MEAN FREE PATH TIME

The concept of mean free path expresses statistically the average distance of the vibrational wave propagation between reflections [2, 18, 19]. For plates, the mean free path can be calculated by [2]

$$d = \pi A/L, \tag{4.1}$$

where $A$ is the surface area of the plate and $L$ is the perimeter of the plate. The energy mean free path time is given as

$$\tau = d/C_g, \tag{4.2}$$

where $C_g$ is the group velocity at which the energy propagates. The energy mean free path time is the mean step length for the change of energy density from one state to another from a statistical point of view. Thus the selection of initial decay slope is constrained by this lower limitation. In other words, in order to see at least two drops of energy flow, the time interval over which a straight line is to be fitted should be at least twice the energy mean free path time. Furthermore, even more energy drops may be required to reduce the

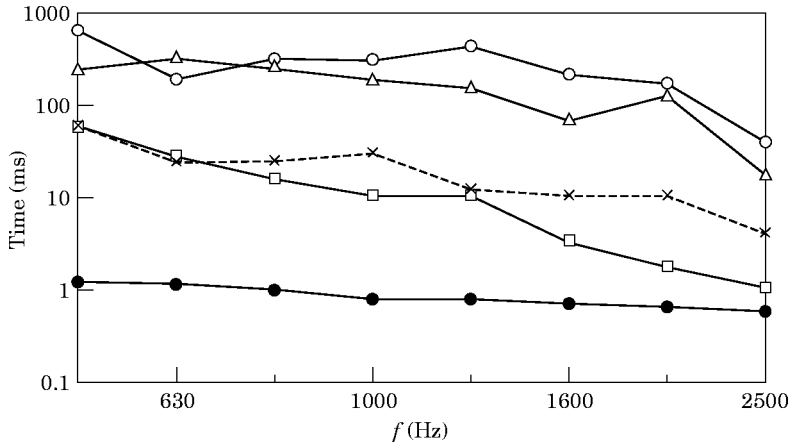


Figure 4. Comparison between energy mean free path time in the plate 1, time intervals for the first 10 dB decay range in the undamped, lightly damped and highly damped plate 1, and space averaged time delay of the initial points of energy decay in the highly damped plate 1. —●—, Energy mean free path time; —○—, time interval for 10 dB decay, undamped; —△—, time interval for 10 dB decay, lightly damped; —□—, time interval for 10 dB decay, highly damped; —×—, time delay of initial decay point, highly damped.

uncertainty of the fitted line due to the various paths of energy flows as mentioned previously.

The energy mean free path time for plate 1 is plotted in Figure 4, together with the time interval for a selected 10 dB decay range for the case of undamped, lightly damped and highly damped plates. The corresponding time interval is calculated by

$$DT_{10} = 10/27{\cdot}3f\eta, \tag{4.3}$$

where $\eta$ is the damping loss factor that is determined by the power input method. It can be seen that for the undamped and lightly damped plates the time intervals for the 10 dB decay range are much larger than the energy mean free path times in all the frequency bands of interest. This indicates that there will be many drops of energy flow in these time intervals which implies that the initial decay slope may be determined in an even shorter time interval or decay interval which is less than 10 dB. Figure 5 shows an example where

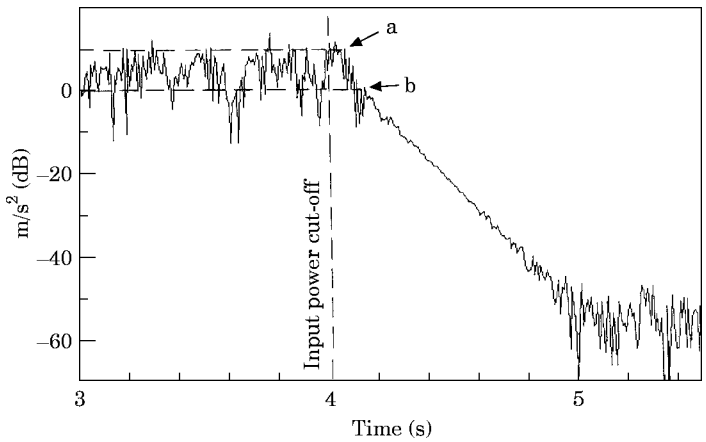


Figure 5. A typical decay envelope in the third octave band of 500 Hz in the highly damped plate 1. 'a' and 'b' are two possible choices of the initial point of the energy decay.

the initial decay slope can be determined within the first 10 dB decay range. For the highly damped case, the time interval over the 10 dB decay range approaches the energy mean free path time with the increase of frequency. They are of the same order of amplitude in the higher frequency range, which implies that the 10 dB decay range may not be wide enough to include at least two energy drops as shown in Figure 3(d). In this case, the decay interval should be extended to at least 20 dB.

It should be noticed that obtaining a true energy decay curve is obscured by the following factors: (i) only the kinetic energy can be measured; (ii) the time resolution in the decay history is limited due to the zoom measurement for the third octave band in the study; the details in the process of energy drop, therefore, cannot be observed precisely. This problem decreases when the bandwidth of the third octave band becomes larger; (iii) the beating phenomenon will modulate the decay envelope when frequencies of two modes are close and damping is very light.

### 4.3. STARTING MOMENT OF ENERGY DECAY

The choice of the starting moment of an energy decay may lead to very different decay slopes. For instance, in Figure 5 use of the initial points 'a' and 'b' will give very different decay slopes. From Figures 3(a–d) and 5, it can be seen that the starting moment of energy decay does not occur when the input power is cut off abruptly. A time delay, $\Delta T_d$, occurs here between the two time instants. Since the average distance between two arbitrarily selected observation and excitation points in a plate should be compatible with the mean free path [2], this implies that the time delay for the drop of the direct energy flow, after the excitation source is suddenly cut off, should be compatible with the energy mean free path time. When the time delay between the moment of power cut-off and the initial point of decay is larger than the energy mean free path time, the decay of energy results from the disappearance of reflected energy flows. Consequently, the energy decay curve includes only the drops of the reflected energy from the reverberant field. In Figures 3(a–d), the observed time delay values for each decay curve are shown.

In a finite plate, the total mean square velocity of vibration is the sum of the direct field and the reverberant field [2]. It was suggested [3] that the direct vibration field should be included in the determination of loss factor of a structure since even for an infinite structure (for which the entire vibration field is "direct"), the ratio $P/\omega E$ in the power input method is still equal to the loss factor. According to these statements, it would follow that a consistency of damping loss factors between the decay rate and the power input methods may be achieved if the initial decay slope includes the first drop of the direct energy flow when the direct field is dominant.

The space averages of observed time delays for the highly damped plate 1 are given in Figure 4. It is shown that the time delays are larger or considerably larger than the energy mean free path times for all the frequency ranges being studied. This indicates that even for the highly damped plate the initial decay point is still governed by the revererant field instead of the direct field. This conclusion is supported by the boundary theory [2] as shown in Figure 6, where the "boundary" between the direct and reverberant field is defined as the distance $\delta$ from the point of excitation and calculated by

$$\delta = f\eta M/\rho C_g, \tag{4.4}$$

when $\eta$ is the damping loss factor that is determined by the power input method, $M$ is the mass, and $\rho$ is the mass per unit area. The range of the direct field around the excitation points is less than 1 cm for the undamped and lightly damped plates 1 and lightly damped plate 2. For the highly damped plate 1 this range is less than 10 cm in most of the frequency bands. In the structures studied, all the randomly selected measurement points were placed

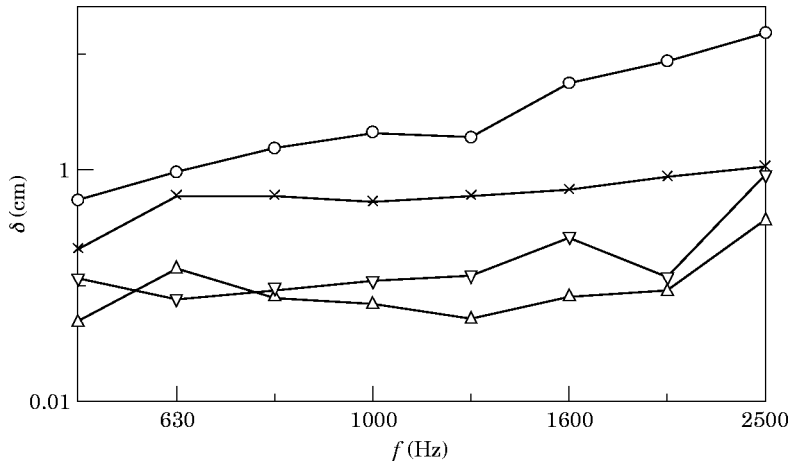


Figure 6. Direct field from the points of excitation in the undamped, lightly damped and highly damped plate 1 and the lightly damped plate 2, which is calculated from equation (4.4). —△—, Undamped plate 1; —▽—, lightly damped plate 1; —○—, highly damped plate 1; —×—, lightly damped plate 2.

at a distance of more than 10 cm from the points of excitation. Thus, the effect of the direct field can be ignored in the study. This indicates that the starting moment of energy decay curves can be considered to occur in the reverberant field. In Figure 5, the point 'a' has a time delay, $\Delta T_d$, equal to 70 ms, which is much larger than the corresponding energy mean free path time (1·26 ms). It can be concluded, therefore, that the point 'a' is already in the reverberation field and should be selected as the initial decay point.

## 5. COMPARISON OF DAMPING LOSS FACTORS BETWEEN THE DECAY RATE AND THE POWER INPUT METHODS

In the study, the mean value of the damping loss factor determined from the power input method for a plate is included by summing up input power and energy separately as given by

$$\eta = \bar{P}/\omega\bar{E}, \tag{5.1}$$

where $\bar{P} = (1/m)\sum_{j=1}^{m} P_j$, $P_j$ is the time averaged input power in the drive point $j$ ($j = 1, \ldots, m$) in the plate, $\bar{E} = M\sum_{j=1}^{m}\sum_{i=1}^{n} v_{ij}^2/nm$, where $v_{ij}^2$ is time averaged square velocity in the measurement point $i$ ($i = 1, \ldots, n$) when the plate is excited in the drive point $j$ and $M$ is the mass of the plate. To calculate the loss factor of a system including two coupled plates, equation (5.1) is still valid if $\bar{E}$ is replaced by the sum of $\bar{E}_1$ and $\bar{E}_2$ for plates 1 and 2, which need to be calculated separately. This type of calculation may be required sometimes in experimental SEA where a subsystem is inhomogeneous.

This type of averaging is based on the assumption of forces that are not correlated at the different driving points. Another type of averaging is to calculate the ratio between input power and energy for each driving point first and then average them over all the driving points. This averaging procedure has, however, been criticized [3] as giving inappropriate weight to areas between modes, where very little vibration energy exists.

For the decay rate method, the mean value of the damping loss factor is estimated by the spatial averaging initial decay rates over a system such as

$$\eta = \bar{\gamma}/27{\cdot}3f, \tag{5.2}$$

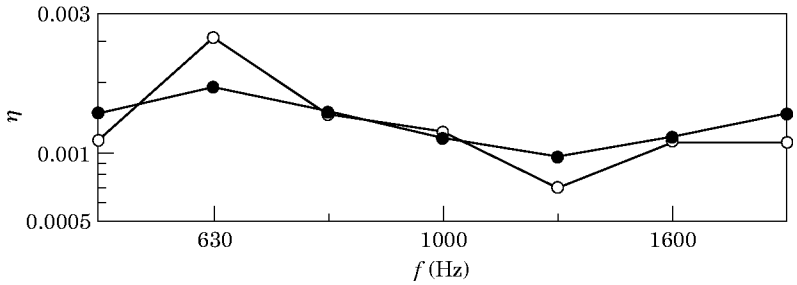


Figure 7. Comparison of damping loss factors obtained by using the decay rate method (—●—) and the power input method (—○—) in the undamped plate 1. Six measurement points and three driving points are used.

where $\bar{\gamma} = \sum_{j=1}^{m} \sum_{i=1}^{n} \gamma_{ij} / nm$ and $\gamma_{ij}$ is the initial decay rate at the measurement point $i$ when the system is excited at point $j$.

For the undamped and lightly damped plate 1, Figures 7 and 8 show that the damping loss factors determined from the two methods in general agree with each other in the frequency bands of interest. For the highly damped plate 1, Figure 9 shows that the damping loss factors using the two methods agree very well in the frequency bands from 500 to 1250 Hz. In the high frequency bands of 1600, 2000 and 2500 Hz, a systematic difference between the two methods can be seen. This problem is in accord with an underlying assumption of equations (2.1) and (2.2): i.e., the decay rate and power input methods are consistent only when damping is light or moderate [3]. The comparison of the damping loss factors determined by the two methods for the system including two coupled plates is shown in Figure 10. A good agreement is achieved between the two methods in all the frequency bands of interest. These comparisons confirm the general conclusion drawn by Jacobsen [3] about the consistency relationship between the decay rate method and the power input method.

## 6. SPATIAL VARIATION ANALYSIS OF INITIAL DECAY RATES

The initial decay rates can show great variation over a surface of a structure. An example of this can be seen in Figure 11 where a measurement on the highly damped plate 1 was carried out in a frequency band which includes several modes. The decay curves 'a' and 'b' were measured at different positions for the same point of excitation. The decay curves 'b' and 'c' were measured at the same position for different excitation points. It is shown

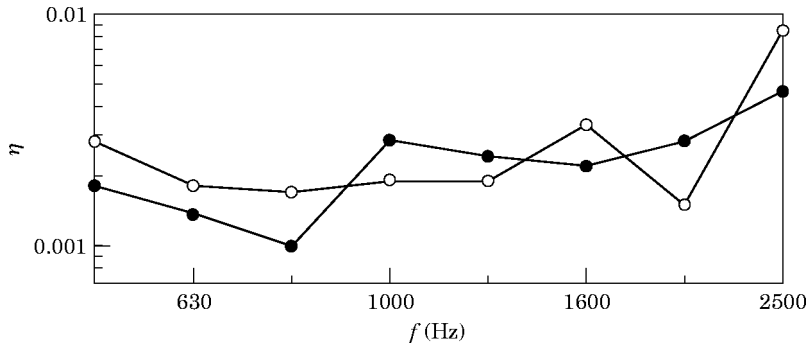


Figure 8. Comparison of damping loss factors obtained by using the decay rate method and the power input method for the lightly damped plate 1. Same number and location of the measurement points and driving points as for the undamped plate 1 are used. Key as Figure 7.

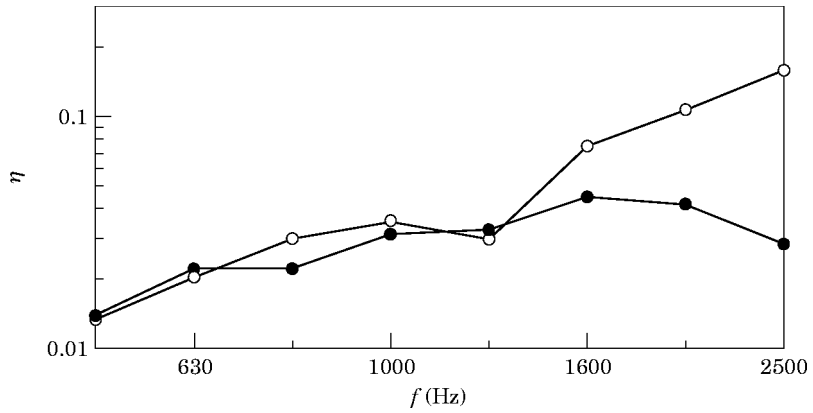


Figure 9. Comparison of loss factors when using the decay rate method and the power input method for the highly damped plate 1. The same number and location of the measurement points and driving points as for the undamped plate 1 are used. Key as Figure 7.

that the initial decay slope is dependent both on the location of the measurement and driving points, which can also be seen for the responses in the power input method [3]. Thus, it is necessary to investigate the spatial variation of the quantity in order to obtain more reliable estimations.

To evaluate the quality in the estimation of initial decay rate, the normalized variance is used as a control measure, which can be calculated by [2, 20]

$$nv = s_d^2 / \overline{d}^2, \tag{6.1}$$

where $\overline{d}$ and $s_d$ are the estimated sample mean and standard deviation. For comparison between different frequency bands and different structural configurations, this relative variance gives more correct information than the variance itself since the mean value may vary with frequency, damping and coupling.

### 6.1. STABILITY OF VARIANCE AND EFFECT OF NUMBER OF MODES

The stability of the normalized variance of the initial decay rates in relation to the number of measurement points is examined under the condition of using three driving points on the undamped plate 1. The data of initial decay rates for 12 randomly selected measurement points are collected. The decay measurements were carried out in seven third octave bands from 500 to 2000 Hz, where the theoretically estimated number of modes per band are from about two to eight as given in Figure 12. For a band that includes only one mode, equation (2.3) shows that the decay slope is independent of the excitation and the measurement locations if these locations are not positioned on the node lines of the

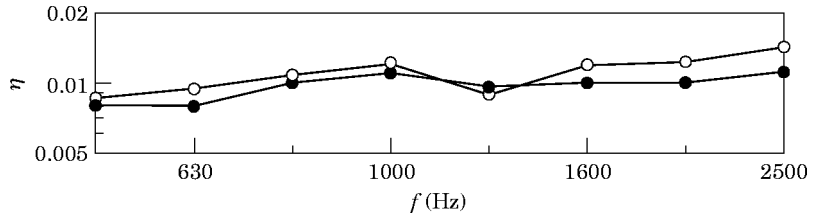


Figure 10. Comparison of loss factors when using the decay rate method and the power input method for a system including two coupled plates 1 and 2. Six measurement points and three driving points for each plate are used. Key as Figure 7.

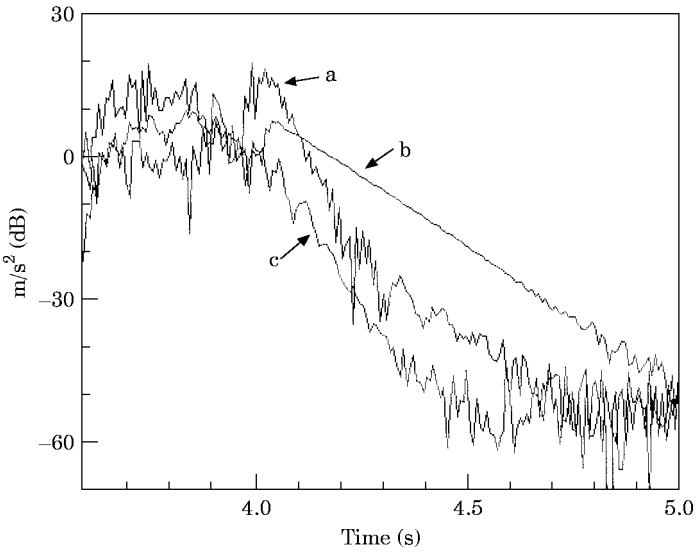


Figure 11. Comparison of energy decay curves in the third octave band of 500 Hz in the highly damped plate 1. Curves 'a' and 'b' are for the different measurement points when using the same driving point. Curves 'b' and 'c' are for the same measurement point when using the different driving points.

mode. The situation is of no interest when the spatial variance of initial decay rate is considered.

A random spatial sampling procedure, with a sample size that increases from 1 to 12, is carried out for the population including 12 measurement points. For each measurement point, there are three values corresponding to three driving points. The variance has been calculated from these three driving points and the measurement points (1–12). In order to avoid occasional chance, this random sampling procedure is run twice and

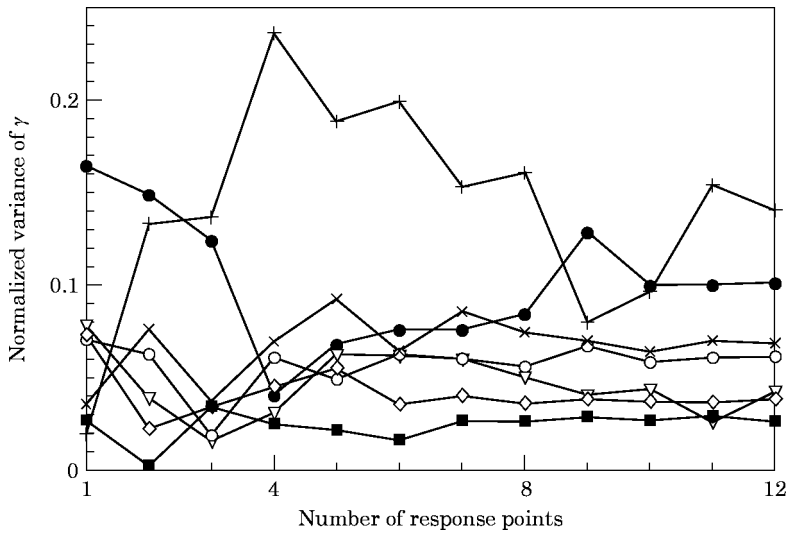


Figure 12. Normalized variances of initial decay rate calculated versus number of the measurement points under the condition of three drive points in the undamped plate 1. $N$: number of modes per band. The data is from the first run of the random sampling procedure. Frequency (Hz), $N$: —●—, 500, 1·87; —○—, 630, 2·38; +, 800, 2·98; —×—, 1000, 3·73; —▽—, 1250, 4·73; —◇—, 1600, 6·03; —■—, 2000, 7·50.

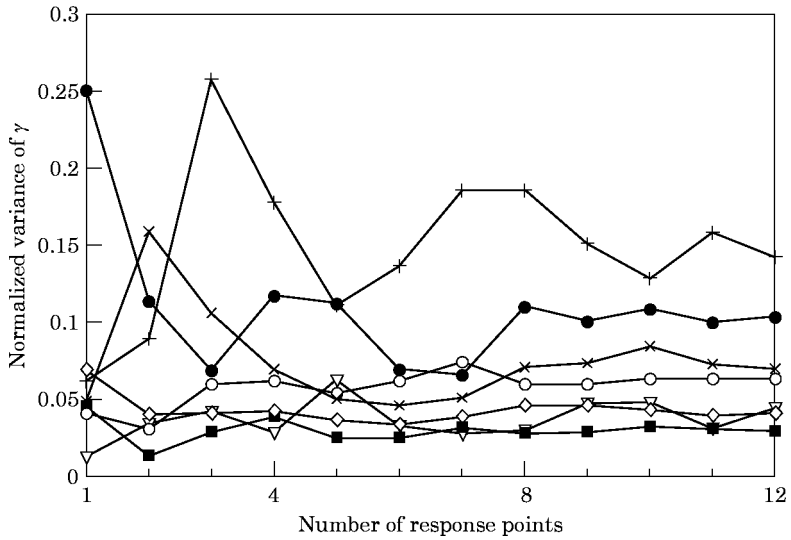


Figure 13. Normalized variances of initial decay rate calculated versus number of the measurement points under the condition of three drive points in the undamped plate 1. The data is from the second run of the random sampling procedure. Frequency key as Figure 12.

the corresponding normalized variances are calculated and plotted versus the number of the measurement points in Figures 12 and 13. It is shown that under the condition of three driving points the normalized variances approach a stable condition more rapidly and have lower values in the high frequency range than in the low frequency range. The curves in the frequency bands of 500 and 2000 Hz show typical examples of this tendency. The damping effect on the normalized variances in the undamped plate can be ignored since the damping loss factors are almost constant over the frequency range of interest as shown in Figure 7. Since the bandwidth and number of modes in a third octave band

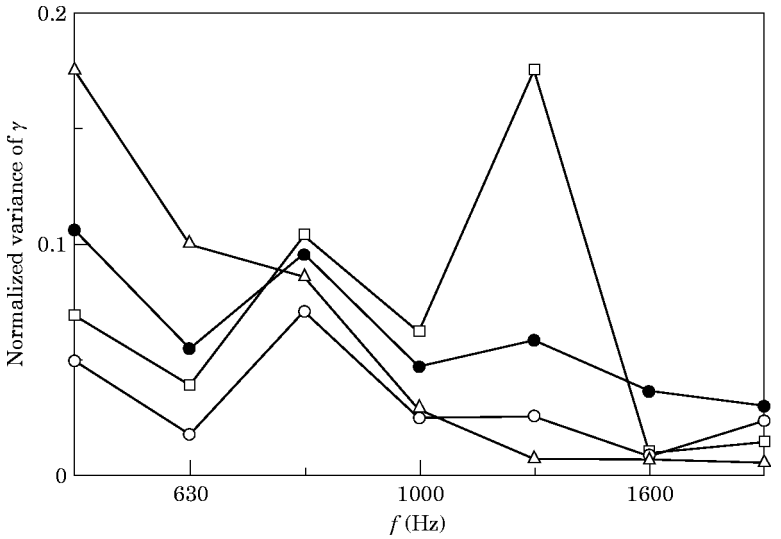


Figure 14. Normalized variances of initial decay rate for each drive point and overall drive points in the undamped plate 1. Six measurement points are used. —○—, Drive point 1; —△—, drive point 2; —□—, drive point 3; —●—, all drive points.

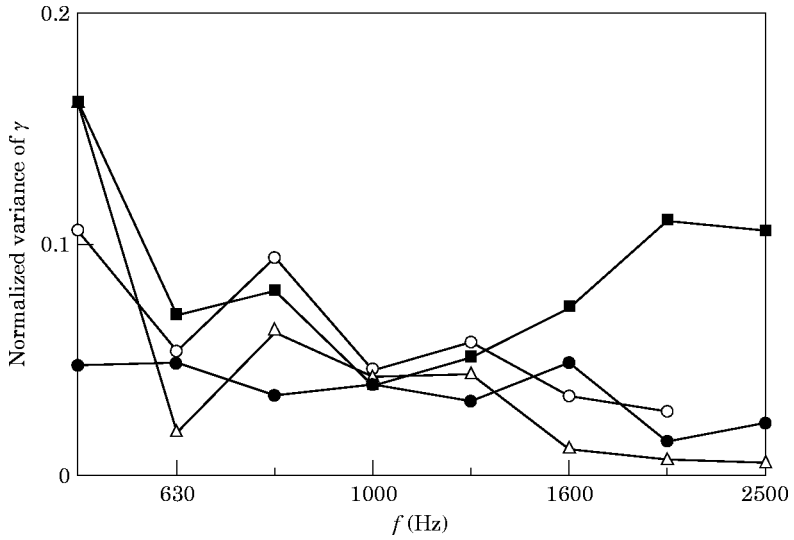


Figure 15. Comparison of normalized variances of initial decay rate for plate 1 in undamped, lightly damped, highly damped, and coupling conditions. Six measurement points are used. —○—, Undamped; —△—, lightly damped; —■—, highly damped; —●—, coupled.

in general increase with frequency, this implies that the increased number of modes in a band can reduce the normalized variance. In addition, for smaller bandwidths where there are few but at least two modes in a band, one needs more randomly selected measurement points to obtain a stable variance estimation. One may also see the effect of the number of modes for the lightly damped plates in Figures 14–16.

### 6.2. EFFECT OF LOCATION OF EXCITATION

Figure 14 gives the normalized variances for each of the three driving points in the undamped plate 1. The data from six randomly selected measurement points out of 12

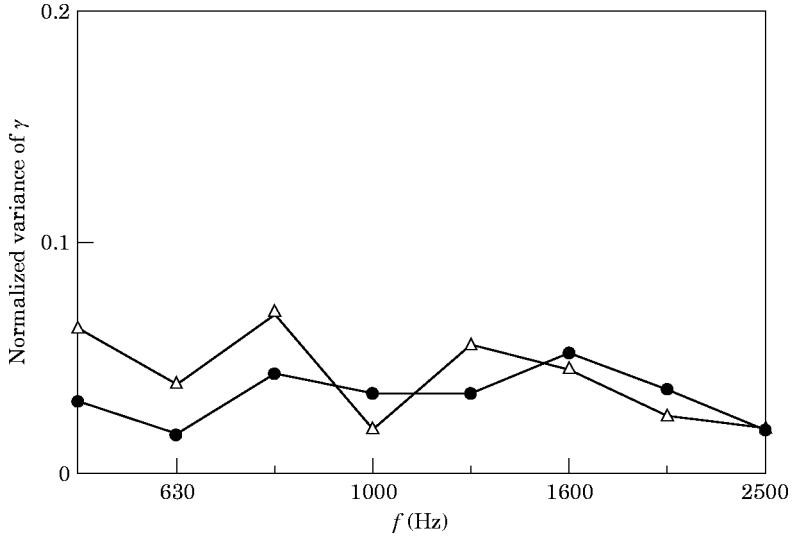


Figure 16. Normalized variances of initial decay rate for plate 2 in lightly damped (—△—) and coupled (—●—) conditions.

measurement points are used. Variations between the normalized variances for different driving points are observed and the normalized variances over all driving points can be larger than that of the individuals, such as those in the bands of 1600 and 2000 Hz. This is because different modes are excited. This finding can also be seen in the cases of lightly damped and highly damped plates.

### 6.3. EFFECT OF DAMPING

The normalized variances of plate 1 in undamped, lightly damped and highly damped conditions are compared in Figure 15. It is shown that the lightly damped plate gives lower normalized variances in most of the frequency range compared to the undamped plate. For the highly damped plate, compared with the undamped and lightly damped cases, the added damping does not reduce the normalized variance in the lower part of frequency range from 500 to 1250 Hz. Furthermore, the added damping increases the normalized variances in the higher part of frequency range from 1600 to 2500 Hz. The explanation may be that (i) such high damping leads to very sharp decay slopes, and as a result calculation of the initial decay rate becomes sensitive to small changes in the positioning of a straight line when determining the initial decay slope, and (ii) for the available decay interval (e.g., 20 dB) the corresponding time interval may not be much larger than the energy mean free path time. This may increase the variation of the initial decay rate.

In the case of two coupled plates, the normalized variances for each plate are given in Figures 15 and 16. It can be seen that the normalized variances are lower in whole the frequency range of interest for both plates. This is mainly because the damping loss factor for each plate is increased to a 'moderate' level due to the coupling damping. It may be concluded that the damping has a positive effect to reduce the space variation of initial decay rate when the damping loss factor is not too high. Comparison of Figures 7–10 and 14–16 shows that this upper limit of damping loss factor is 0·03 or 0·04.

### 6.4. INTERVAL OF STANDARD DEVIATION

Figures 17 and 18 give the mean values and standard deviations of the initial decay rates for the lightly damped and highly damped plate 1. It is found that the intervals of standard deviation are approximately proportional to the mean values. This is logical from a statistical point of view since the standard deviation is based on deviations from the mean. Larger deviations would be expected from a large mean than from a small one. In practice, this proportion corresponds to that the initial decay rate is more sensitive to small variations in the selection of initial decay slope when the frequency or damping increases, because the initial decay rate is proportional to the damping loss factor and frequency in terms of equation (2.1).

Figure 19 presents the same results but on a log scale. It is shown that the intervals of standard deviation of the initial decay rate on a log scale are comparable to the related normalized variances as given in Figure 15. This is because both the quantities deal with relative values.

## 7. COMPARISON OF NORMALIZED VARIANCES BETWEEN THE DECAY RATE AND THE POWER INPUT METHODS

For a uniform plate, the formula of variance of damping loss factor determined from the power input method in equation (5.1) can be expressed as

$$s_\eta^2 = (1/\omega \bar{V}^2 M)^2 s_P^2 + (\bar{P}/\omega(\bar{V}^2)^2 M)^2 s_{V^2}^2, \tag{7.1}$$

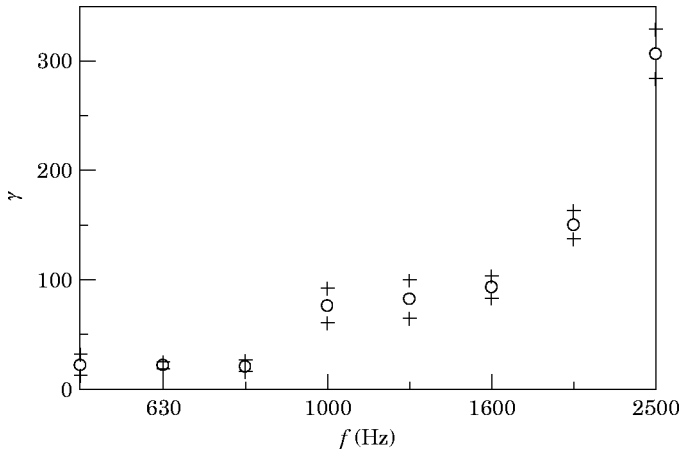


Figure 17. Mean values (○) and standard deviation intervals (+) for plate 1 in lightly damped condition. The data are plotted on a linear scale.

where $V^2$ and $P$ are the variables of time averaged squared velocity and input power, $\bar{V}^2$ and $\bar{P}$ are the spatial averages of time averaged squared velocity and input power, and $s^2_{V^2}$ and $s^2_P$ are the sample variances of time averaged squared velocity and input power. The details of derivation of equation (7.1) by using the theory of propagation of error [21, 22] is given in Appendix 1. This theory has been applied to a previous work on statistical and sensitivity aspects of the power input method [23].

Equation (7.1) shows that the variances of loss factor refers to two sources of variances: that is, the variation of input power due to the location of driving points and the variation of squared velocity due to both location of driving points and measurement points.

The comparison of the normalized variances of damping loss factor determined from the decay rate and the power input methods is given in Figures 20 and 21 for the undamped and highly damped plate 1. This comparison is reasonable since the mean values of damping loss factor determined from these two methods agree reasonably well with each other as shown previously, even though the compared quantities are from two different populations. For the highly damped plate, this comparison is performed only in the

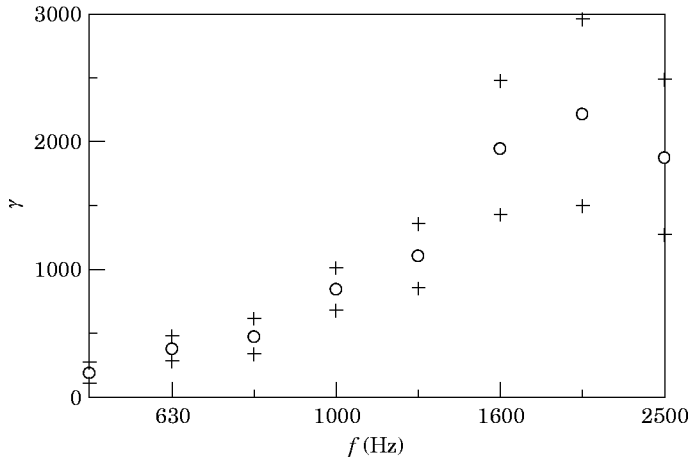


Figure 18. Mean values and standard deviation intervals of initial decay rate for plate 1 in highly damped condition. The data are plotted on a linear scale. Key as Figure 17.

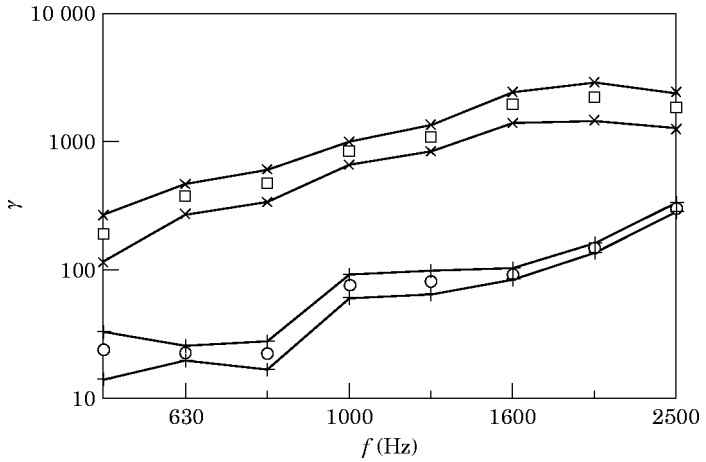


Figure 19. Mean values and standard deviation intervals of initial decay rate for plate 1 for lightly damped and highly damped conditions. The data are plotted on a log scale. ○, Mean, lightly damped; +, 1 std, lightly damped; □, mean, highly damped; —×—, 1 std, highly damped.

third octave bands from 500 to 1250 Hz since systematic differences of the mean values of damping loss factor appear between the two methods in the higher frequency range as shown in Figure 9. It is shown that for the plates investigated the normalized variances of damping loss factors determined by using the decay rate method are much lower than those of damping loss factor determined by using the power input method in all the third octave bands of interest for both undamped and damped situations. This indicates that with the same location of driving and measurement points, the decay rate method will produce more reliable estimates of damping loss factor than the power input method. Figures 20 and 21 show also that the source of variance due to velocity has larger contributions to the total normalized variance than that due to input power.

Equation (7.1) is an approximation. If the error due to truncation of the Taylor series is taken into account, the actual variances of damping loss factors may be higher than those given by equation (7.1). This is, however, still consistent with the previous conclusion.

## 8. FINAL REMARKS

In this study, the initial decay rate of energy decay curves has been studied experimentally on single, coupled, undamped, and damped rectangular plates. The purpose is to obtain a better understanding of the process of the initial decay, to investigate the spatial variation of the initial decay rate in order to obtain more reliable estimation of the loss factor determined from the decay rate method, and to compare the spatial averages and spatial variances between the decay rate method and the power input method.

The main conclusions can be drawn as follows.

(i) The concept of the energy free path time is useful in characterizing the initial decay stage. Principally, the time interval for the initial decay slope should be at least twice (even much larger than) that of the energy mean free path time. It is concluded that the initial decay slopes can sometimes be selected within a very short decay interval (e.g., less than 10 dB) provided that the principal above is fulfilled. Accordingly, the dimension and damping of a structure as well as frequency are the factors that influence the determination of an initial decay slope.

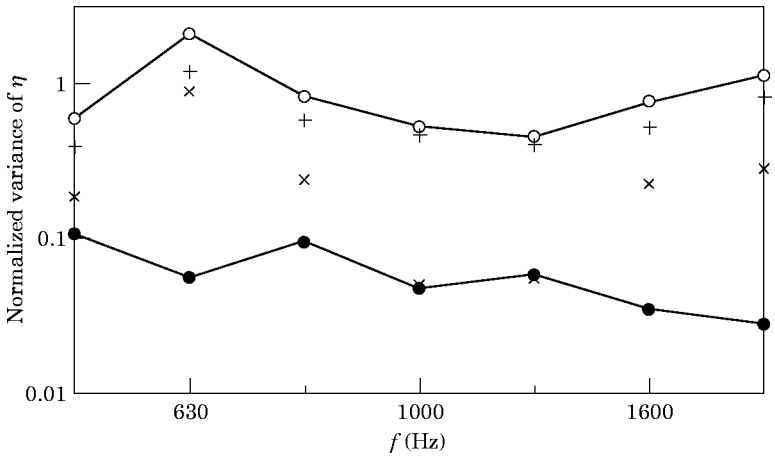


Figure 20. Comparison of normalized variances of damping loss factor determined when using the decay rate method and the power input method for plate 1 for the undamped condition. The variance of damping loss factor determined by using the power input method is calculated by equation (7.1). —○—, Power input method, total; ×, power input method, due to input power; +, power input method, due to velocity; —●—, decay rate method.

(ii) It is observed that the starting point of decay of energy is delayed a time period from the instance when the input power is suddenly switched off. The time delay can also be quantified by the energy mean free path time. It can be concluded that only the energy decay in the reverberant field should be considered when the measurement points are not close to the driving points. It should be noted that the size of the direct field is dependent on the physical size of a structure.

(iii) It is confirmed that the loss factors obtained when using the decay rate and the power input methods agree with each other for undamped, lightly damped, highly damped plates (up to a specific frequency) and coupled plates.

(iv) The analysis of spatial variation of initial decay rate shows that for a frequency band with few, but no less than two, modes more measurement points need to be used to obtain a stable estimation of variance.

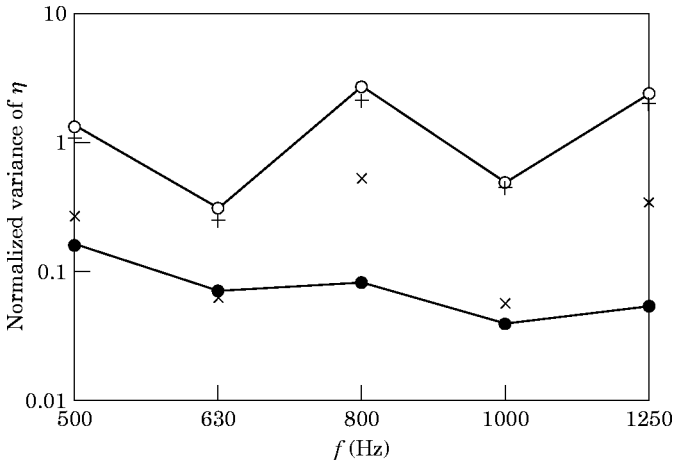


Figure 21. Comparison of normalized variances of damping loss factor determined when using the decay rate method and the power input method for plate 1 in a highly damped condition. The variance of damping loss factor determined by using the power input method is calculated by equation (7.1). Key as Figure 20.

(v) The increase of number of modes in a frequency band and the increased damping reduces the spatial variation of the estimates of initial decay rate. However, too high damping may increase the spatial variation. This limit for damping loss factor is about 0·03 or 0·04 in the study.

(vi) For single plates, the normalized variances of damping loss factor determined from the decay rate method are much less than those determined from the power input method. This suggests that for a certain number of driving and measurement points, the decay method should be the first choice when determining a reliable estimate of damping loss factors compared to the power input method. In addition, in the power input method, the spatial variation of velocity contributes more to the total variance of estimates of damping loss factor than that of input power.

## ACKNOWLEDGMENTS

Acknowledgment is made to two referees of this paper for their valuable comments.

## REFERENCES

1. E. E. Ungar 1992 in *Noise and Vibration Control Engineering*, *Principles and Applications* (edited by L. L. Beranek and I. L. Ver), Chapter 12: Structural damping. New York: John Wiley.
2. R. H. Lyon and R. G. DeJong 1995 *Theory and Application of Statistical Energy Analysis*. MA: Butterworth-Heinemann; second edition.
3. F. Jacobsen 1986 *Technical University of Denmark Report No*. 41. Measurement of structural loss factors by the power input method.
4. S. Gade and H. Herlufsen 1990 *Proceedings of the 8th International Modal Analysis Conference*. Digital filter technique versus FFT techniques for damping measurements.
5. D. A. Bies and S. Hamid 1980 *Journal of Sound and Vibration* **70**, 187–204. *In situ* determination of loss and coupling loss factors by the power injection method.
6. M. F. Ranky and B. L. Clarkson 1983 *Journal of Sound and Vibration* **89**, 309–323. Frequency average loss factors of plates and shells.
7. F. J. Fahy 1969 *Journal of Sound and Vibration* **9**, 507–508 (Letter to the Editor). Reply to the Letter to the Editor "Damping in plates" by M. J. Crocker and A. J. Price.
8. J. C. Sun and E. J. Richards 1985 *Journal of Sound and Vibration* **103**, 109–117. Prediction of total loss factors of structures, Part I: Theory and experiments.
9. J. C. Sun, H. B. Sun, L. C. Chow and E. J. Richards 1986 *Journal of Sound and Vibration* **104**, 243–257. Predictions of total loss factors of structures, Part II: loss factors of sand-filled structures.
10. G. Maidanik 1977 *Journal of Sound and Vibration* **52**, 171–191. Some elements in statistical energy analysis.
11. M. P. Norton and R. Greenhalgh 1986 *Journal of Sound and Vibration* **105**, 397–423. On the estimation of loss factors in lightly damped pipeline systems: some measurement techniques and their limitations.
12. P. V. Bruël 1978 *B&K Technical Review*, *No*. 3. The enigma of sound power measurements at low frequencies.
13. H. Larsen 1978 *B&K Technical Review*, *No*. 4. Reverberation processes at low frequencies.
14. J. S. Bendat and A. G. Piersol 1993 *Engineering Applications of Correlation and Spectral Analysis*. New York: John Wiley; second edition.
15. M. R. Schroeder 1965 *The Journal of the Acoustical Society of America* **37**, 409–412. New method of measuring reverbation time.
16. M. R. Schroeder 1979 *The Journal of the Acoustical Society of America* **66**, 497–500. Integrated-impulse method measuring sound decay without using impulses.
17. F. Jacobsen and D. Bao 1987 *Journal of Sound and Vibration* **115**, 512–537. Acoustic decay measurements with a dual channel frequency analyzer.
18. L. L. Beranek 1988 in *Noise and Vibration Control* (edited by L. L. Beranek). Chapter 8: Sound in small spaces. Washington, DC: Institute of Noise Control Engineering; revised edition.

19. L. CREMER, H. A. MULLER and T. J. SCHULTZ 1982 *Principles and Applications of Room Acoustics*, Volume 1. London: Applied Science Publishers.
20. A. D. MOHAMMED 1990 *Institute of Sound and Vibration Research*, *University of Southampton Ph.D. Thesis*. A study of uncertainty in applications of statistical energy analysis.
21. R. M. BETHEA, B. S. DURAN and T. L. BOULLION 1995 *Statistical Methods for Engineers and Scientists*. New York: Marcel Dekker, INC., third edition, revised and expanded.
22. J. A. RICE 1995 *Mathematical Statistics and Data Analysis*. California: Wadsworth Publishing Company; second edition.
23. K. D. LANGHE 1996 *Department of Mechanical Engineering*, *Katholieke University of Leuven Ph.D. Thesis*. High frequency vibrations: contributions to experimental and computational SEA parameter identification techniques.

## APPENDIX A

The variance of loss factor determined by using equation (5.1) can be derived from the theory of propagation of error [21, 22].

For a non-linear function $Y = f(X_1, X_2, \ldots, X_n)$ with independent random variables $X_1, X_2, \ldots, X_n$, the dependent variable $Y$ can be linearized approximately by applying a Taylor series expansion about the point $\mu = (\mu_1, \mu_2, \ldots, \mu_n)$ where $\mu_i = \mathrm{E}(X_i)$. One has

$$f(X_1, X_2, \ldots, X_n) \cong f(\mu_1, \mu_2, \ldots, \mu_n) + \sum_{i=1}^{n} \left( \left. \frac{\partial f}{\partial X} \right|_{X_i = \mu_i} \right) (X_i - \mu_i). \tag{A1}$$

Recalling that if $U = a + bW$, where $a$ and $b$ are constant, then $\sigma_U^2 = b^2 \sigma_W^2$, one has

$$\sigma_Y^2 \cong \left( \left. \frac{\partial f}{\partial X_1} \right|_{X_1 = \mu_1} \right)^2 \sigma_{X_1}^2 + \left( \left. \frac{\partial f}{\partial X_2} \right|_{X_2 = \mu_2} \right)^2 \sigma_{X_2}^2 + \cdots + \left( \left. \frac{\partial f}{\partial X_n} \right|_{X_n = \mu_n} \right)^2 \sigma_{X_n}^2. \tag{A2}$$

In equation (5.1), the time averaged input power $P$ and the time averaged squared velocity $V^2$ are two independent variables when the random noise excitation is used. Thus, the variance of loss factor can be expressed as

$$s_\eta^2 \cong (1/\omega \bar{V}^2 M)^2 s_P^2 + (\bar{P}/\omega (\bar{V}^2)^2 M)^2 s_{V^2}^2, \tag{A.3}$$

where $\bar{P} = 1/m \sum_{j=1}^{m} P_j$, $P_j$ is the time averaged input power at the drive point $j$ ($j = 1, \ldots, m$) in the plate, $\bar{V}^2 = \sum_{j=1}^{m} \sum_{i=1}^{n} V_{ij}^2 / mn$, $V_{ij}^2$ is the time averaged square velocity in the measurement point $i$ ($i = 1, \ldots, n$) when the plate is excited in the drive point $j$, $M$ is the mass of the plate, $s^2$ replaces $\sigma^2$ since the sample variance is used to estimate the unknown population variance, $s_P^2 = \sum_{j=1}^{m} (P_j - \bar{P})^2/(m-1)$ and $s_{V^2}^2 = \sum_{j=1}^{m} \sum_{i=1}^{n} (V_{ij}^2 - \bar{V}^2)^2/(mn-1)$.